Self-Consistent Brownian Dynamics Simulation of Bimodal Polymer Brushes under Shear

Marina G. Saphiannikova,* Victor A. Pryamitsyn, and Tatiana M. Birshtein

Institute of Macromolecular Compounds, Russian Academy of Sciences, 31 Bolshoi pr., V.O., 199004 St. Petersburg, Russia

Received July 13, 1999; Revised Manuscript Received December 22, 1999

ABSTRACT: The method of self-consistent Brownian dynamics developed recently has been adapted to simulate the properties of bimodal polymer brushes under shear. Simulations of three systems with different compositions have been carried out for a range of shear rate values. In the absence of shear, the free ends of short and long chains are mostly found in different sublayers inside the brush. Similar to the collapse of monodisperse brushes, we observed under shear a collapse of the outer sublayer, which is composed of long chains. Short chains are not stretched and inclined if the shear is not strong enough to cause a considerable intermixing of their free ends with the free ends of long chains in the direction perpendicular to the grafting surface. When the shear becomes very strong such intermixing occurs, and all chains are stretched and inclined in the shear direction. The number of chains, directly affected by shear, is very small. However, the shear stress is transferred into the brush below the flow penetration level owing to the rotation of the free chain ends.

1. Introduction

This study is a follow-up of the investigation of the behavior of polymer brushes in strong shear flows.[1] A polymer brush represents an important example of an interfacial polymer layer when molecules are end-grafted to an impenetrable surface. Polymer layers are very important as a tool to modify surface properties. These layers have many technological applications, e.g., steric stabilization and flocculation of colloidal dispersions, selective membrane modifications, chromatography, lubrication, adhesion, etc.[2]

Properties of monodisperse polymer brushes under shear have been intensively studied theoretically for the past few years. Both analytical studies using mostly the scaling theory[3−8] and different methods of computer simulation[1,9−15] were applied to solve the problem.

Detailed analysis of previous computer simulation studies, carried out in ref 1, revealed that in the most cases the values of the shear stress were relatively small. Under these conditions the brush height and the extension ratio of polymer chains change only slightly with the shear rate. Recently we developed a novel computer simulation method, named self-consistent Brownian dynamics,[1] which allows us to study the properties of polymer brushes in strong shear flows.

It was found that the brush height strongly decreases when the shear stress is high enough to stretch the chains so that their lengths in the lateral direction become comparable with the contour length (Gaussian threshold). In the process of brush collapse under shear, the polymer density profiles and distributions of free ends change in the same manner as observed during compression of the brush[16] or during brush collapse in a poor solvent.[17] It was shown that the shear flow directly affects only the brush periphery, pulling inside the layer those free ends that are the farthest from the grafting surface. The distribution of free-end velocities gives evidence that the diffusion of the free chain ends in the direction normal to the grafting surface causes a diffusive penetration of the shear stress into the brush below the flow penetration level. As a result, chains that are not directly affected by the flow are found also to be inclined in the flow direction.

In ref 1 only monodisperse polymer brushes composed of chains having the same length were studied. Polymers are always polydisperse, and the effects of polydispersity within a grafted layer can be quite severe. To analyze these effects we chose as a model a bimodal system, namely, a polymer brush composed of chains with two different lengths.

As was shown previously using SCF theory,[16,18] at equilibrium the free ends of each species are confined in distinctive layers of the bimodal brush. Moreover, bimodal distribution of the free ends is also retained for the bimodal brush under compression. Therefore, we expected a suppression of the vertical diffusion of the free ends in a bimodal brush if it is compressed by shear. This means the diffusive transfer of shear stress into the bimodal brush should also be suppressed and the average conformations of short chains should be perpendicular to the grafting surface.

It will be shown in the present paper that for small shear stresses such behavior is really observed. However, if the shear stress is very high, the free-end distribution function is no longer bimodal. A destruction of the original bilayer structure of the bimodal brush occurs owing to a diffusive transfer of the shear stress into the inner sublayer, which is composed of short chains.

2. Brush Model

The brush is represented by an assembly of polymer molecules, end-grafted to an impenetrable surface. The brush structure is determined by a self-consistent molecular field and a self-consistent shear flow. A freely jointed chain is chosen as the model for the polymer molecule. There are two types of chains inside the brush: short ones with a number of segments equal to N_1 and long ones with a number of segments equal to N_2. We introduce as a parameter the relative difference between the chain lengths, $\alpha = (N_2 - N_1)/N_1 > 0$. The fractions of short and long chains will be designated

10.1021/ma9911400 CCC: $19.00
Published on Web 03/16/2000

Table 1. Characteristics of the Systems

system	N_1	N_2	α	q_1	q_2
A	80	180	1.25	0.8	0.2
B	80	130	0.625	0.6	0.4
C	50	150	2.0	0.5	0.5
M	100	0	0.0	1.0	0.0

below as q_1 and $q_2 = 1 - q_1$, respectively. The first bead of every chain is placed at the origin of the local Cartesian coordinate system with the x-axis parallel to the direction of the shear flow and the y-axis perpendicular to the grafting surface.

Three systems with different compositions are studied in the present work (see Table 1). The values of two parameters are chosen equal to those describing the monodisperse brush in our previous study:[1] the dimensionless grafting density (number of polymer chains per unit area), $\sigma = 0.1$, and the average number of segments in a chain, $N = 100$, ($N = N_1q_1 + N_2q_2$). The monodisperse brush will be indicated below as system M.

3. Self-Consistent Brownian Dynamics Method

The Brownian dynamics algorithm used in the present study is fully described in our previous paper concerning simulation of monodisperse brushes under shear.[1] It is governed by a system of Langevin equations describing the motions of chain beads:

$$\vec{F}^{(l)}_{\text{react}} + \vec{F}^{(l)}_{\text{b}} + \vec{F}^{(l)}_{\text{h}} + \nabla\vec{U}_{\text{mf}}(\vec{r}_l) = 0, \quad l = 1, 2, ..., N \quad (1)$$

The tensions in the segments, $\vec{F}^{(l)}_{\text{react}}$, which serve to conserve the segment length a, are given by

$$\vec{F}^{(l)}_{\text{react}} = -\frac{\partial U(\vec{b}_l)}{\partial \vec{r}_l} - \frac{\partial U(\vec{b}_{l+1})}{\partial \vec{r}_l}, \quad U(\vec{b}_l) = K\left(\vec{b}_l^{\,2} + \frac{1}{\vec{b}_l^{\,2}}\right) \quad (2)$$

where $\vec{b}_l = \vec{r}_l - \vec{r}_{l-1}$ is a bond vector and $\vec{r}_l$ is the position vector of chain bead l. The value of the elastic coefficient K was chosen large enough ($K = 80k_BT$) to provide a fixed bond length until very high stretching.

$\vec{F}^{(l)}_{\text{b}}$ represents the random Brownian force to which bead l is subjected. For polymer models, with a constant friction coefficient of segments, the mean value of the Brownian force $\langle\vec{F}^{(l)}_{\text{b}}\rangle = 0$ and $\langle(\vec{F}^{(l)}_{\text{b}})^2\rangle = (6k_BT/\zeta)\Delta t$.

The hydrodynamic force is described as

$$\vec{F}^{(l)}_{\text{h}} = \zeta\left\{\vec{V}(\vec{r}_l(t)) - \frac{\partial\vec{r}_l(t)}{\partial t}\right\} \quad (3)$$

where $V(\vec{r}_l(t))$ is the average local flow velocity. In our case of pure shear flow, it is equal to $V_x(y(t))$, and $\partial\vec{r}_l(t)/\partial t$ is the velocity of bead l at time t.

The last term in the Langevin equations represents the gradient of the molecular field potential. The local exchange chemical potential of the polymer chains, $\mu(y)$, is used as the potential of the molecular field similar to that in Scheutjens−Fleer self-consistent field theory:[19]

$$U_{\text{mf}}(y) = \mu(y) = -ln(1 - \rho(y)\cdot a^3) \quad (4)$$

All equations were solved numerically in the dimensionless form. The segment length a, energy k_BT, and bead friction coefficient ζ are chosen as basis units so that the unit of time is $\tau = \zeta a^2/k_BT$. Here k_B is the Boltzmann constant and T is the absolute temperature. The second-order trapezoidal method with one iteration and a time step $\delta t = 0.0005\tau$ was used for the integration.

To reduce computer time, we chose a representative assembly of 100 polymer molecules, which all have different initial conformations and are all affected by different stochastic forces but are placed in the same external molecular field. Thus, in our study both volume and hydrodynamic interactions between the polymer segments are considered self-consistently.

The shear flow is calculated by using the Brinkman equation[20]

$$\frac{d^2V_x(y)}{dy^2} = \frac{\zeta}{\eta}\rho(y)\,V_x(y) + \frac{\Delta p}{\eta} \quad (5)$$

where $V_x(y)$ is the velocity of the shear flow, $\rho(y)$ is the brush density profile, Δp is the pressure gradient (for pure shear $\Delta p = 0$), and η is the viscosity of the solvent. The friction coefficient, ζ, is related to η through Stokes' law $\zeta = 3\pi\eta a$.

We introduce the dimensionless shear stress

$$\varpi = \frac{\gamma\eta a^3}{k_BT} \quad (6)$$

where γ is the shear rate.

The boundary conditions are

$$V_x(y)|_{y=0} = 0, \quad \frac{\eta a^3}{k_BT}\frac{dV_x}{dy}|_{\rho=0} = \varpi \quad (7)$$

The self-consistent procedure can be described by the following equation

$$\rho_i(y) = \text{BD}\{U_{\text{mf}}[\rho_{i-1}(y)],\, V_x[\rho_{i-1}(y)]\} \quad (8)$$

where BD is a symbolic name of the Brownian dynamics procedure that accumulates the density profile, $\rho_i(y)$, determining the molecular field and the shear velocity, $V_x(y)$, for the next iteration, i. The number of time steps per iteration was equal to 100.

As was shown by Barrat,[5] additional stretching of the chains in the brush under weak shear deformation results in an increase of the repulsive volume interactions between monomers. The origin of this effect is due to local density fluctuations and is related to a weakening of volume interactions screening the stretched chains. As a result, the osmotic pressure inside the brush under weak shear deformation grows, which causes an increase of the brush thickness. Therefore, the swelling of the polymer brush predicted by scaling studies[5−7] cannot be verified in mean-field approaches that neglect local density fluctuations, including ours.

Doyle et al.[13] utilized a Brownian dynamics algorithm that included explicit calculations of volume interactions between polymer segments and a self-consistent procedure for the calculation of the average shear flow. This was calculated from the Brinkman equation (eq 5) using the average density profile accumulated during one iteration step. Previously we found a good agreement between density profiles calculated by the self-consistent Brownian dynamics method and obtained from ref 13 at the same values of ϖ.[1] This means that the self-consistent approximation is quite adequate to describe volume interactions in polymer brushes under shear.

We intend to study the behavior of bimodal polymer brushes in strong shear flows. When the shear force per chain does not exceed the Gaussian threshold $fa/k_BT \sim 1$, the chains behave like springs with constant elasticity and we deal with a weak flow. It was shown previously,[1] for a monodisperse brush with $\sigma = 0.1$, the crossover between weak and strong flows occurs when $\varpi > 0.01$ and does not depend on the length of the polymer chains.

A bimodal brush at equilibrium consists of two distinct layers.[16,18] The free ends of short chains are found to be in the inner layer and those of long chains in the outer layer of the brush. The outer layer can be roughly treated as a monodisperse brush with the grafting density, σ_2, equal to $q_2\sigma$. It was predicted by Milner[3] and confirmed in our study[1] that the shear flow only slightly penetrates inside the monodisperse brush owing to the flow modification effects. One can expect that only the free ends of the long chains in the outer layer will be stretched at the start of the shear flow. On the other hand, the flow will be less screened by the polymer molecules owing to the smaller density of the outer layer. As a result, at the same values of the dimensionless shear stress, ϖ, and the grafting density, σ, shear will affect the long chains in a bimodal brush much more than those in a monodisperse brush. In principle, decreasing q_2 we can achieve a free-draining situation for the outer layer when flow modification effects become negligible, and the short chains will be already directly affected at the start of the shear flow.

Owing to restrictions in the chosen model (see eq 2), the contour length of long chains could not be conserved for very strong flows. Therefore, we chose for the simulation of the bimodal polymer brushes the range $0 \le \varpi \le 0.4$. We performed detailed simulations of system B at $\varpi = 0$, 0.05, 0.1, 0.2, and 0.4. Systems A and C were studied only in the absence of shear and at $\varpi = 0.4$. First, we have applied the shear flow with $\varpi = 0.4$ to equilibrium brush structures. It takes about 30 000 iterations to attain the stationary state, and 6000 iterations are used to accumulate average distribution functions. In the case of system B, the following runs for lower shear rates were started using as an initial state the chain conformations obtained at the next higher shear rate. Such a reduced procedure is quite applicable because, as was shown previously,[1] two stationary brush structures obtained from different initial conformations, independently starting from higher or lower shear rates, are identical.

4. Results

Density Profiles and Free-End Distributions. We obtained the overall brush density profile, $\rho(y)$, and the distributions of the free ends of short chains, $g_1(y)$, and long chains, $g_2(y)$, in the direction perpendicular to the grafting surface. These functions are normalized as follows:

$$\int_0^\infty \rho(y)\,dy = N\sigma, \quad \int_0^\infty g_i(y)\,dy = q_i, \quad i = 1, 2 \qquad (9)$$

Figure 1 shows the influence of the shear flow on system B. The density profile changes in the same manner as observed in the process of collapse of the monodisperse brush under shear.[1] That means the profile contracts toward the grafting surface and becomes a steplike function. The distribution of the free ends of short chains practically does not change with an increase of the shear rate, but that for the long chains becomes narrower and sharper while moving toward the surface. This leads to a significant increase of the crossover area where the free chain ends of the different species intermix. Owing to the much lower statistics of the free-end distribution functions, they show no smooth curves such as density functions but a wigglelike structure.

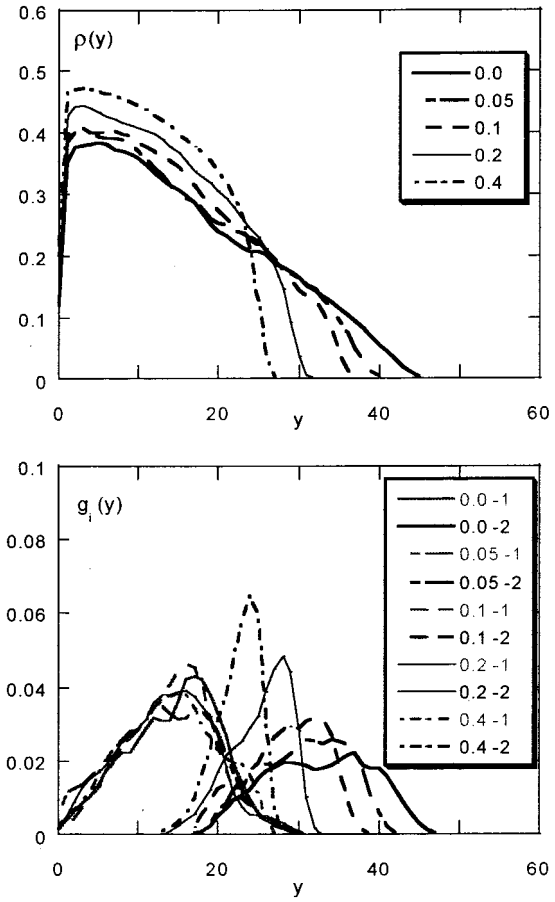

Figure 1. Set of density profiles and free-end distribution functions for system B at different ϖ values. The gray lines correspond to the short chains, and the black ones correspond to the long chains.

The process of collapse of the bimodal brush was also controlled by estimating the following moments of distribution functions:

$$R_y^2 = \frac{\int_0^\infty y^2 \rho(y)\,dy}{N\sigma} \qquad (10)$$

$$h_i^2 = \frac{1}{q_i}\int_0^\infty y^2 g_i(y)\,dy, \quad i = 1, 2 \qquad (11)$$

Here R_y is the mean-square height of the segments and h_1 and h_2 are the mean-square heights of the free ends of short and long chains in the brush, respectively. The dependencies of R_y, h_1, and h_2 vs dimensionless shear stress ϖ are shown in Figure 2. R_y and h_2 decrease approximately one and a half times under shear, while h_1 keeps the same value equal to the equilibrium one. Thus, such a picture confirms that in the case of collapse of the bimodal brush under shear there are the long chains that are compressed.

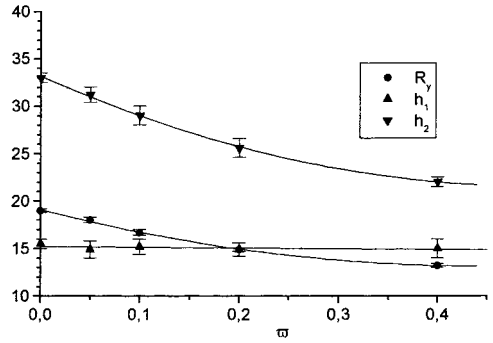

Figure 2. R_y, h_1, and h_2 vs dimensionless shear stress ϖ.

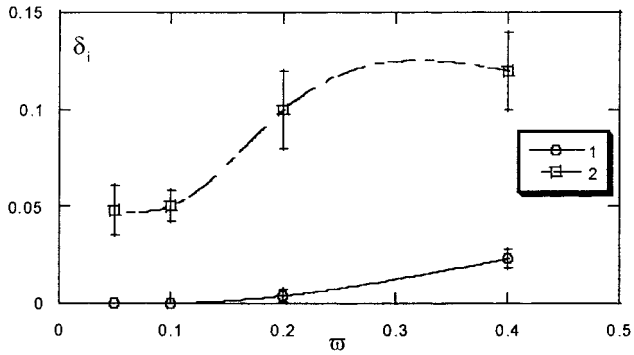

Figure 3. Fractions of short and long chains directly affected by the shear flow vs dimensionless shear stress ϖ for system B.

The fractions of short and long chains, directly affected by the shear flow, are given by[1]

$$\delta_i(\varpi) = \frac{\int_0^\infty g_i(y)\,\rho(y)\,V_x(y)\,dy}{\int_0^\infty \rho(y)\,V_x(y)\,dy}, \quad i = 1, 2 \qquad (12)$$

Here $V_x(y)$ is the velocity of the shear flow. It is clearly seen from Figure 3 that in system B short chains are not directly affected by the shear flow at $\varpi \leq 0.2$. With the increase in ϖ δ_1 slightly increases, which gives for the highest shear rate in our study less than 2% of short chains, directly affected by shear (1 of 60). On the contrary, the corresponding fraction of long chains, δ_2, increases with shear stress gradually. But still at $\varpi = 0.4$ the number of long chains, directly affected by shear, is very small and does not exceed 12% (5 of 40).

Figure 4 shows the influence of the shear flow on the density profile, $\rho(y)$, for bimodal brushes with different compositions. In the absence of shear, an equilibrium structure of bimodal brushes differs significantly from that of the monodisperse brush. The density profile of the latter has a parabolic form, while the density profile of bimodal brushes represents itself a broken line composed of two regions. The crossover between the regions corresponds to an area where the free ends of short and long chains intermix (see Figure 5).

To show that our results are very reliable, let us compare for the case of the absence of shear a system calculated using the mean-field theory from ref 16, which is very similar to the system B. In both cases the same brush composition is considered, $q_1 = 0.6$, but the relative difference of chain lengths is a bit lower in analytical studies, $\alpha = 0.6$. The density profiles normalized by the procedure described in ref 16 fit together rather well except for a small gap near the grafting

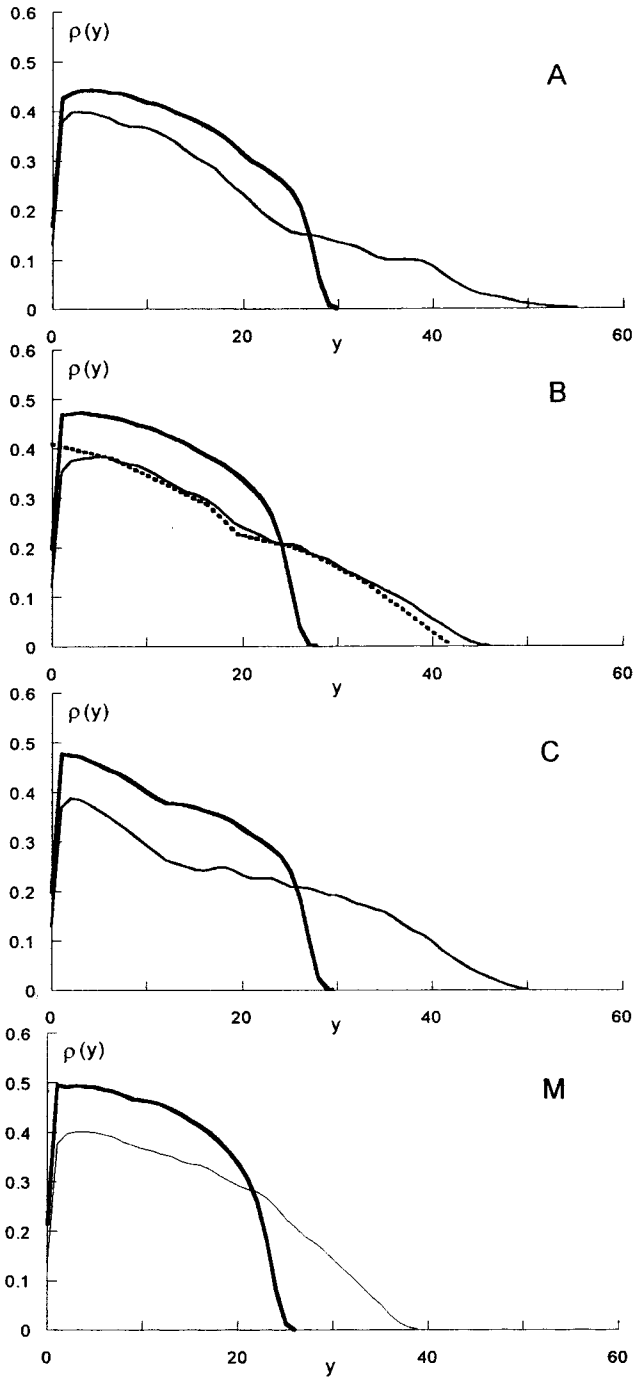

Figure 4. Set of density profiles of the bimodal brushes (A, B, C) and the monodisperse brush (M) in the absence of shear (thin line) and under shear (thick line) with $\varpi = 0.4$. The dashed line corresponds to the equilibrium density profile of a system calculated in ref 16, which is very similar to system B.

surface and a short tail (Figure 4). It is known that both regions could not be properly described by the mean-field theory. The crossover region predicted analytically is very well reproduced in self-consistent Brownian dynamics simulations.

In the process of collapse of bimodal brushes under strong shear, the density profiles change in a different way depending on the system composition. In the case of systems A and B with low relative difference between chain lengths, α, they become steplike functions. These profiles are similar to those obtained for the monodisperse brush under strong shear. In the case of system

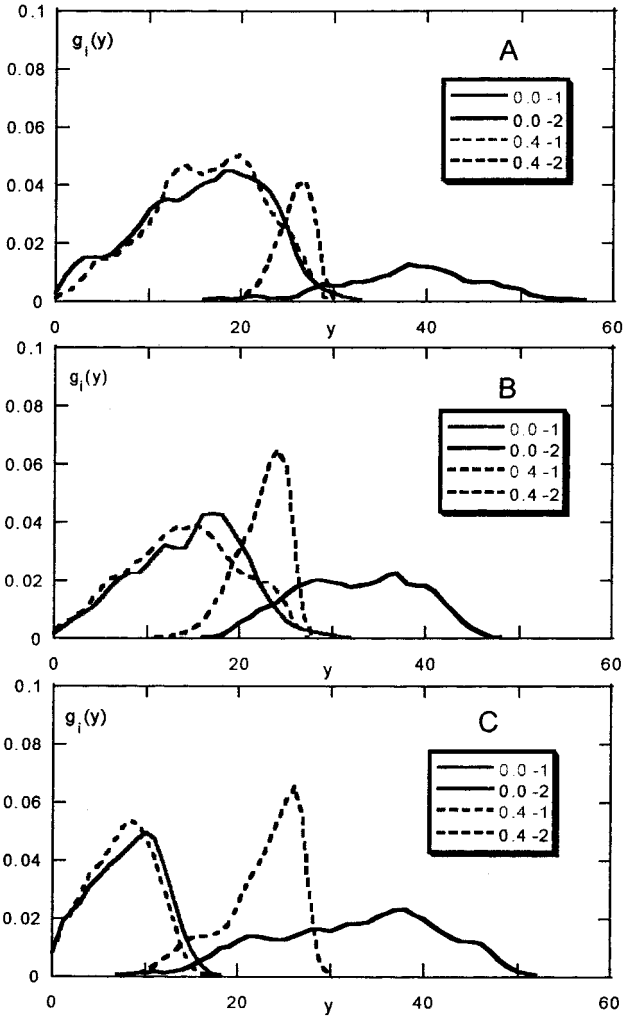

Figure 5. Set of free-end distributions for the short (gray lines) and long chains (black lines) in the bimodal brushes with different compositions (see Table 1) at $\varpi = 0$ and 0.4.

C with a higher $\alpha = 2.0$, one can still distinguish between two regions in the compressed density profile, which represents a slightly broken line. All bimodal brushes are thicker than the monodisperse one at any value of shear rate. This can be explained by the presence of long chains with $N_2 > N$.

In the absence of shear the free ends of short and long chains are mostly found in different sublayers inside the brush (Figure 5). Only a small fraction of the free ends of short (long) chains penetrates into the outer (inner) sublayer. Under shear the free ends of long chains are forced to go closer to the grafting surface. It is the outer sublayer that is compressed by the shear flow. The free ends of short chains practically are not redistributed in the direction perpendicular to the grafting surface, and the contraction of the inner sublayer seems to be negligible for all three systems. This leads to a significant increase of the crossover area, especially pronounced for systems A and B (Figure 5), where at $\varpi = 0.4$ the outer sublayer totally disappears. In this case all free ends of long chains intermix with the free ends of short chains. The behavior of system C is slightly different, which can be clearly seen from Figure 5. Here the outer sublayer is so thick and dense in the absence of shear that a flow with $\varpi = 0.4$ is not strong enough to destroy the initial bilayer structure.

Thus, the behavior of bimodal brushes at equilibrium and under shear strongly depends on their composition. There are two independent parameters, α and q_1, describing it. If fractions of short and long chains are comparable in magnitude, $q_1 \approx q_2$, then with the increase in α a more pronounced bilayer structure will be observed. Long chains in such systems should totally screen the inner layer of short chains up to very strong shear flows with $\varpi = 1$. On the contrary, with the decrease in α a difference in the lengths of short and long chains will gradually become negligible. The already investigated case of monodisperse brush under shear will be approached. This means that shear flows with $\varpi \sim 0.1$ will affect chains of both lengths.

If we keep α constant, then at small q_1 strong shear flows will affect only the upper layer of the long chains. With an increase in q_1 one will gradually achieve the free-draining situation for this layer. It was shown in ref 15 that a simple shear flow with $\varpi \sim 0.001$ is sufficient enough in the free-draining case to compress a monodisperse brush. Thus, at high q_1 the upper layer will be quickly compressed at relatively small shear rates and then the contraction of the inner layer composed of short chains will begin at $\varpi \sim 0.1$. This case should also resemble the monodisperse situation.

Unfortunately, we can give only a qualitative picture in this paper, as a careful mapping of the whole (α, q_1, ϖ) parameter space presents an unsolvable simulation task demanding huge computational resources.

Average Conformations. The free ends of polymer chains in the equilibrium monodisperse brush are distributed over the entire brush extent.[21] But if the free end of a polymer chain in a specific thin layer of the brush is fixed, the fluctuations of the other segments are minimized.[21] In other words, the only fluctuations in the equilibrium brush are the free-end fluctuations. So the inner brush structure can be represented as average conformations of chains with their free ends found in different layers inside the brush. Such a representation proved to be very informative for the monodisperse brush under shear.[1] It was shown, for example, that chains with their free ends found near the grafting surface do not feel the flow at all and behave like a Gaussian coil. The chains with their free ends found near the brush periphery are stretched and inclined in the shear direction. Such a detailed picture of the inner brush structure could not be observed if only one average is calculated for all chains in the brush.

Let us recall how these average chain conformations are obtained. The space near the grafting surface is divided into thin layers parallel to the surface. The width of each layer is equal to $2.5a$. Then the conditional distribution functions $T_x(x, l, m)$ and $T_y(y, l, m)$ are accumulated. They describe the probabilities that the lth bead has the coordinates x or y when the free end of a chain is found in the mth layer. The average trajectories reconstructed from the conditional distribution functions represent the sequences of points, $(\langle x_l \rangle, \langle y_l \rangle)$, $l=0, 1, ..., N$, with $\langle y_N \rangle \in [2.5ma, 2.5(m+1)a]$, $m = 0, 1, ..., 19$.

We have calculated average conformations for short and long chains separately. Figure 6 shows the set of average conformations at $\varpi = 0.1, 0.2, 0.4$ for system B. One can see that the shear flow with $\varpi = 0.1$ strongly affects the long chains that are stretched and inclined along the x direction (Figure 6a). Short chains do not feel the flow with this ϖ at all. Their average conformations are vertical. With the increase in shear rate, the

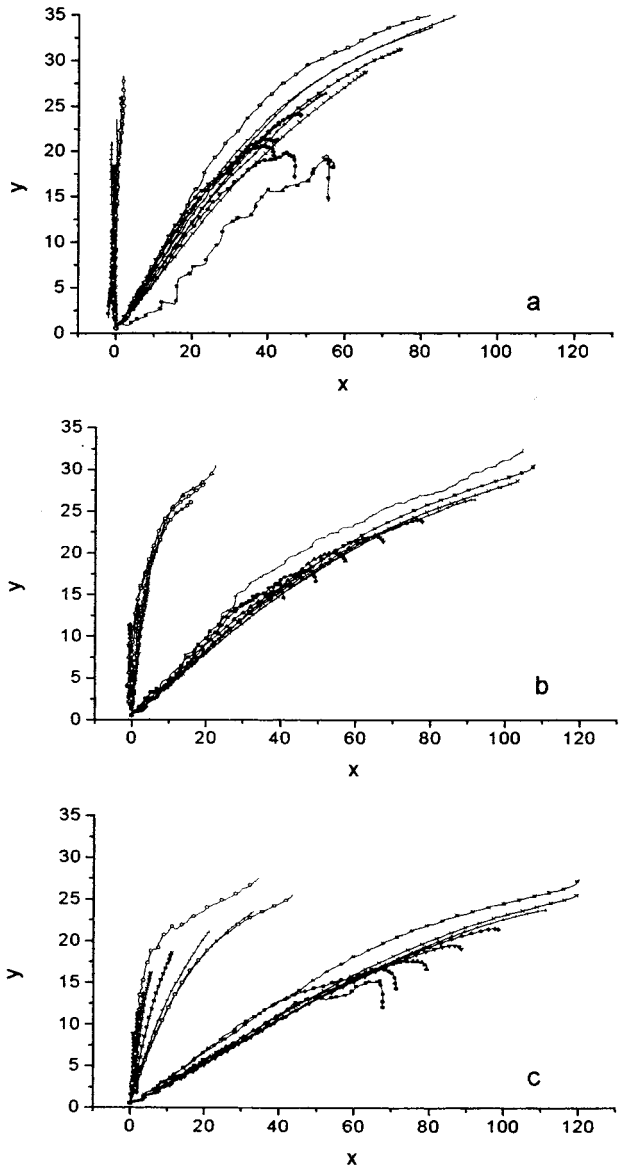

Figure 6. Set of average conformations at $\varpi = 0.1$ (a), 0.2 (b), and 0.4 (c) for system B.

degrees of stretching and inclination of long chains gradually increase. The ends of short chains directly affected by the shear flow become also slightly inclined. However, this inclination does not cause a redistribution of their free ends in the direction perpendicular to the grafting surface (see Figure 1b).

One might expect that the average conformations of long chains with their ends directly affected by the flow should be inclined, and ones situated below the flow penetration level should be vertical. Figure 6 shows, however, a very unusual effect. The average conformations of long chains situated below the zone of direct influence of the flow are also inclined. After the end of a long chain has penetrated the flow zone, the chain starts to be stretched by the shear flow. When the stretching exceeds the Gaussian threshold, the chain stiffens. This changes the balance between elasticity and osmotic pressure, and the chain contracts toward the surface. Since the stretching is now reduced, the stress continuously relaxes and the chains become less stiff. Finally, the osmotic pressure will force the long chain away from the surface. In Figure 6 the average conformations corresponding to the stiffened chains are represented by almost straight lines, and those corresponding to the relaxed chains have slightly coiled ends.

The data for system A at $\varpi = 0.4$ are qualitatively similar with those in Figure 6c, but the degree of inclination of long chains is higher because the outer layer in system A is less dense than the outer layer in system B (see Figure 4). As a result the shear flow is less screened by the polymer molecules in system A. The degree of inclination of short chains is slightly smaller because the inner layer is more dense in comparison with system B. The data for system C at $\varpi = 0.4$ resembles those in Figure 6a. As was told previously, the short chains in this system do not feel the strong flow at all, being covered by the dense layer of long chains. Therefore, the average conformations of short chains are found to be vertical.

As was discussed above, we have found a diffusive penetration of the shear stress into the monodisperse brush below the flow penetration level.[1] This was explained by the diffusion of the free chain ends in the direction normal to the grafting surface. It is known that in polydisperse mixtures of chains vertical diffusion of the free ends of the polymer chains is suppressed.[22] So we expect that the diffusive transfer of shear stress into the inner sublayer of short chains also will be suppressed. To illustrate the location of a diffusion flow in the bimodal brush (system B), we have drawn a picture of the 2-dimensional free-end distribution functions, $g_i(x, y)$, $i = 1, 2$, for short and long chains, and the free-end flow (Figures 7 and 8).

It is clearly seen that only the free ends of long chains are involved in a rotational flow. There is an uncompensated shear force at the outer border of the brush and an uncompensated x-component of the elastic force just below the flow penetration level. There are only two regions where all three forces acting on the polymer chains are approximately in equilibrium. These regions correspond to the local maxima of the 2 -dimensional free-end distribution function found at $\varpi = 0.2$ around the points (65, 22) and (115, 28) (Figure 7).

As was expected, the vertical diffusion of the free ends of short chains is totally suppressed. At $\varpi < 0.2$, the shear flow does not penetrate into the inner sublayer of the bimodal brush and does not affect directly the free ends of short chains (Figure 7). Only when some fraction of short chains becomes directly affected by shear with $\varpi \sim 0.4$ (Figure 8) could the structure of the inner sublayer be slightly changed (Figure 6c). The behavior of long chains is very similar to that observed for polymer chains in the monodisperse brush.[1] Their free ends rotate in the xy-plane causing a diffusive penetration of shear stress. With the increase in ϖ the velocity of this rotation increases. Contrary to the short chains, all long chains are inclined and stretched including those that are not directly affected by the shear flow. Thus, our hypothesis seems to be confirmed in the present simulation studies.

5. Discussion

It was shown previously[1] that in the process of collapse of a monodisperse brush under shear the polymer density profiles and distributions of the free ends change in the same manner as observed during compression of the brush.[16] The density profiles change from parabolic to steplike ones, and the free-end distributions become sharper. Thus, strong shear flows affect the monodisperse brush like a compressing wall.

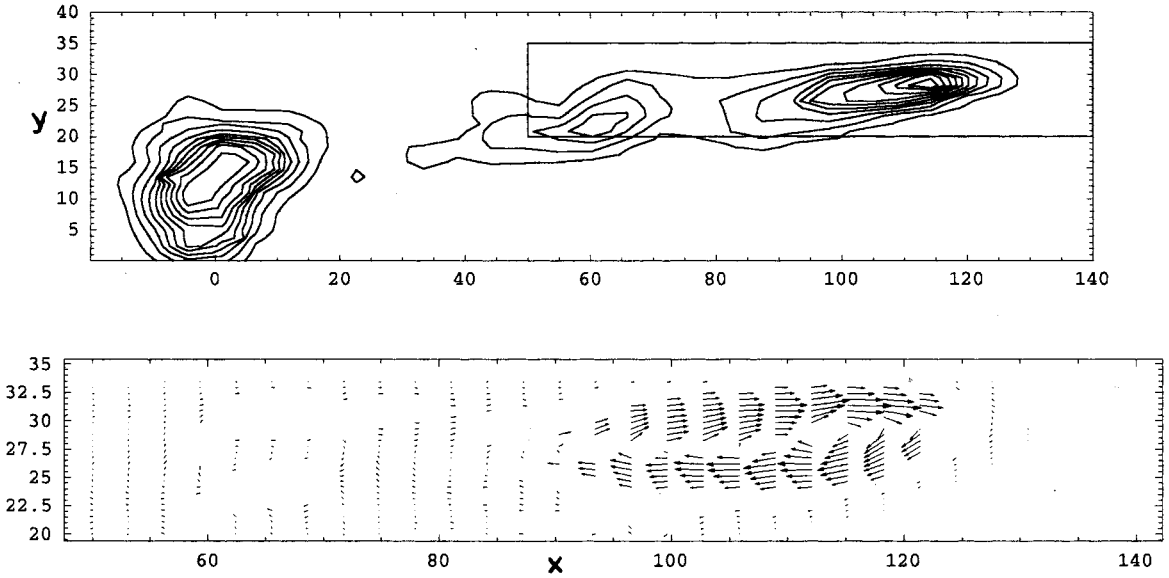

Figure 7. Two-dimensional free-end distribution function for the short and long chains (upper diagram) and a rotational flow of the free ends (lower diagram). The length of the arrows of the lower diagram corresponds to an average value of the velocity of the free-end diffusion. System B; $\varpi = 0.2$.

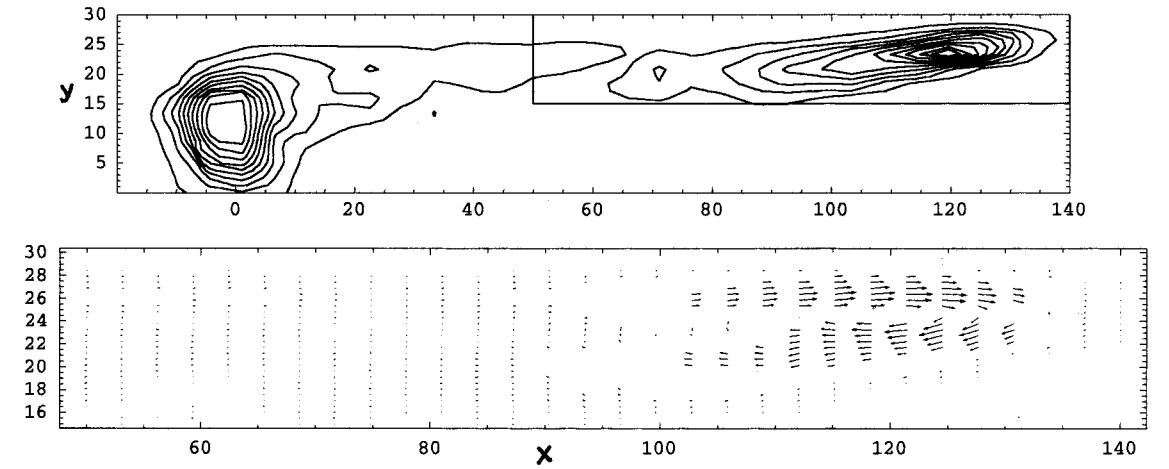

Figure 8. Two-dimensional free-end distribution function for the short and long chains (upper diagram) and a rotational flow of the free ends (lower diagram). The length of the arrows of the lower diagram corresponds to an average value of the velocity of the free-end diffusion. System B; $\varpi = 0.4$.

Two regions can be distinguished in the density profiles of the bimodal brushes compressed by a wall. They correspond to the sublayers of the short and long chains. The free-end distributions of both species turned out to be sharper in this case. Therefore, a simultaneous contraction of both sublayers in bimodal brushes under a compressing wall was predicted in ref 16 assuming that both sublayers are highly stretched in the absence of compression.

A totally different picture is observed for the bimodal brushes subjected to strong shear flows. The density profiles change from broken to a steplike function, and only the free-end distribution of long chains becomes narrower and sharper. The free ends of short chains practically are not redistributed in the direction perpendicular to the grafting surface, and contraction of the inner sublayer seems to be negligible for all studied systems. These data show that it is the outer sublayer that is compressed by the shear flow.

A wall compressing the bimodal brush in the normal direction acts on both layers. The minimum of free energy corresponds to the situation where the free ends of different species avoid each other, assuming the relative difference between their lengths is large enough.[16] On the contrary, the shear flow slightly penetrating inside the brush affects only its periphery. It is the finite extensibility of polymer chains that is responsible for a decrease in the brush thickness under strong shear flows. At weak shear an increase of the chain dimension in the flow direction occurs without any variation in the component normal to the grafting surface (Gaussian or linear regime). The chains should be highly stretched in the lateral direction by shear (nonlinear regime) before a significant decrease of the brush height could be observed. Thus, a strong shear flow effectively contracts the chain lengths in the direction normal to the grafting surface. On the contrary, extension ratios of the chains inside a brush compressed by a wall decrease: the free ends of long chains going down under compression make the free ends of short chains go closer to the grafting surface.[16] One can see the inner brush structures are quite different in these two cases, although density profiles

and free-end distribution functions are very similar for the compressed and sheared monodisperse brushes.

6. Conclusions

In the present study a self-consistent Brownian dynamics method previously developed for monodisperse brushes under shear was adopted to study equilibrium and nonequilibrium structures of bimodal brushes. Despite some simplifications, the method again proved itself to be a reliable and powerful technique.

It is confirmed that at equilibrium the density profile of bimodal brushes is composed of two regions.[16,18] In the process of collapse under shear, it becomes a steplike function. Similar density profiles were obtained for the monodisperse brush.[1]

In the absence of shear, the free ends of short and long chains are mostly found in different sublayers inside the brush. It is the outer sublayer that is compressed by the shear flow. If the shear is not strong enough to cause a considerable intermixture of the free chain ends of the different species in a vertical direction, then the short chains cannot be stretched and inclined. Under strong shear flow such intermixing occurs and already all chains are stretched and inclined in the shear direction. At this stage not only long chains but also some of the short ones participate in the rotational flow.

The number of long chains, directly affected by shear, is very small. However, owing to the rotation of their free ends shear stress is transferred below the flow penetration level. We have observed the same picture for the monodisperse brush in a previous study.[1]

We conclude that although the collapse of monodisperse brush under shear resembles its behavior during compression by a wall the process of collapse of bimodal brush under shear differs significantly from its compression.[16] Shear causes a destruction of the original bilayer structure of the brush that remains under compression.

Acknowledgment. We acknowledge support from RFBR (Grants 99-03-33319 and 96-15-97401).

References and Notes

(1) Saphiannikova, M. G.; Pryamitsyn, V. A.; Cosgrove, T. *Macromolecules* **1998**, *31*, 6662.
(2) Fleer, G. J.; Cohen Stuart, M. A.; Scheutjens, J. M. H. M.; Cosgrove, T.; Vincent, B. *Polymers at Interfaces*; Chapman and Hall: London, 1993.
(3) Milner, S. T. *Macromolecules* **1991**, *24*, 3704.
(4) Rabin, Y.; Alexander, S. *Europhys. Lett.* **1990**, *13*, 49.
(5) Barrat, J.-L. *Macromolecules* **1992**, *25*, 832.
(6) Birshtein, T. M.; Zhulina, E. B. *Macromol. Chem. Theory Simul.* **1992**, *1*, 193.
(7) Harden, J. L.; Cates, M. E. *Phys. Rev. E* **1996**, *53*, 3782.
(8) Harden, J. L.; Borisov, O. V.; Cates, M. E. *Macromolecules* **1997**, *30*, 1179.
(9) Grest, G. S. In *Dynamics in Small Confined Systems III;* Drake, J. M., Klafter, J., Kopelman, R., Eds.; Materials Research Society: Pittsburgh, PA, 1997; Vol. 464.
(10) Grest, G. S. *Adv. Polym. Sci.* **1999**, *138*, 149.
(11) Lai, P.-Y.; Binder, K. *J. Chem. Phys.* **1993**, *98*, 2366.
(12) Lai, P.-Y.; Lai, C.-Y. *Phys. Rev. E* **1996**, *54*, 6958.
(13) Doyle, P. S.; Shaqfeh, E. S. G.; Gast, A. P. *Phys. Rev. Lett.* **1997**, *78*, 1182.
(14) Miao, H.; Guo, H.; Zuckermann, M. *Macromolecules* **1996**, *29*, 2289.
(15) Neelov, I. M.; Borisov, O. V.; Binder, K. *Macromol. Theory Simul.* **1998**, *7*, 141.
(16) Birshtein, T. M.; Liatskaya, Yu. V.; Zhulina, E. B. *Polymer* **1990**, *31*, 2185.
(17) Zhulina, E. B.; Borisov, O. V.; Pryamitsyn, V. A.; Birshtein, T. M. *Macromolecules* **1991**, *24*, 140.
(18) Milner, S. T.; Witten, T. A., Cates, M. E. *Macromolecules* **1989**, *22*, 853.
(19) Scheutjens, J. M. H. M.; Fleer, G. J. *J. Phys. Chem.* **1979**, *83*, 1619.
(20) Brinkman, H. C. *Appl. Sci.* **1947**, *A1*, 27L.
(21) Milner, S. T. *Science* **1991**, *251*, 905.
(22) Klushin, L. I.; Skvortsov, A. M. *Macromolecules* **1992**, *25*, 3443.

MA9911400